GEOLOGY

Decadal-scale shifts in soil hydraulic properties as induced by altered precipitation

Joshua S. Caplan[1,2], Daniel Giménez[1]*, Daniel R. Hirmas[3], Nathaniel A. Brunsell[4], John M. Blair[5], Alan K. Knapp[6]

Soil hydraulic properties influence the partitioning of rainfall into infiltration versus runoff, determine plant-available water, and constrain evapotranspiration. Although rapid changes in soil hydraulic properties from direct human disturbance are well documented, climate change may also induce such shifts on decadal time scales. Using soils from a 25-year precipitation manipulation experiment, we found that a 35% increase in water inputs substantially reduced infiltration rates and modestly increased water retention. We posit that these shifts were catalyzed by greater pore blockage by plant roots and reduced shrink-swell cycles. Given that precipitation regimes are expected to change at accelerating rates globally, shifts in soil structure could occur over broad regions more rapidly than expected and thus alter water storage and movement in numerous terrestrial ecosystems.

INTRODUCTION

Soil hydraulic properties govern the movement of water into and out of the rhizosphere; they determine the fraction of rainfall that infiltrates versus runs off, regulate the availability of water for uptake by plants, and constrain rates of evaporation and transpiration. As such, they are fundamental components of land surface models (1). Despite their influence on water cycling at the largest spatial scales, soil hydraulic properties are determined by the size distribution, connectivity, and total volume fraction of soil pores, with large pores having a disproportionately strong influence on soil water fluxes (2). During the process of soil formation, precipitation regimes and other climatic factors shape soil hydraulic properties by moderating both abiotic and biotic processes (e.g., mineral weathering and decomposition of organic matter) (3–5). These changes are well documented on century to millennial time scales, with the implication that shifts in soil hydraulic properties are generally considered to be long-term processes (6). Where rapid shifts have been documented, they have been associated almost exclusively with direct physical or chemical alteration to soil such as tillage, deforestation, or fertilizer use (1, 7, 8).

We posit that changes in precipitation regimes could induce appreciable alterations in mean soil hydraulic properties over shorter time scales (i.e., years to decades) and across broad regions if processes that control soil structure are sufficiently malleable in response to altered soil moisture levels. A number of physical, chemical, and biological processes have strong and synergistic effects on soil pore systems (9, 10) and may therefore be able to induce decadal-scale shifts in response to altered precipitation. For instance, root biomass and diameter can change as plant communities undergo succession or transition in response to changing environmental conditions (11, 12); growing root systems are known to variously create new pores, colonize existing pores, reduce pore sizes as they displace and compact soil, and release exudates that contribute to macroaggregate formation (10, 13). In addi-

tion, sustained changes in shrink-swell cycles can alter pore structure by rearranging clay particles (10) and multi-week periods of saturation or rapid wetting of dry soil can alter soil aggregation (14). The cumulative effect of such processes over years to decades can condition or delay the responsiveness of soil to subsequent environmental change (15).

Evidence that anthropogenic climatic changes can induce decadal-scale shifts in soil structure and hydraulic properties is sparse but mounting. For instance, changes in soil porosity, aggregate stability, and water retention have been documented in response to elevated concentrations of atmospheric CO_2 (16–18). Also, warmer temperature regimes can be deleterious to aggregate stability, particularly in dry soils (19). Shifts induced by altered precipitation regimes are likewise poorly described, although continental-scale variation in precipitation has been associated with changes in soil macroporosity (20) and intense drought can increase water retention in organic soils (15). On the basis of this evidence and the relatively rapid rates of the above-mentioned mechanisms, we predicted that a change in mean annual rainfall could likewise yield appreciable changes in soil hydraulic properties and do so in one to two decades.

Our investigation centered on a field experiment that ran for more than 25 years in an annually burned tallgrass prairie in the Central Plains of North America (table S1) (21). In this experiment, known as the irrigation transect experiment (ITE), a 35% increase in mean annual precipitation (Fig. 1A) was implemented via sprinkler irrigation on two of four transects along a hillslope (7-m elevation difference over 140 m). The timing and duration of irrigation events was calibrated such that water inputs would approximate potential evapotranspiration by plants and soils through the growing season (Fig. 1B), thus minimizing temporal dynamics while maximizing soil water content. This replicated, long-term experiment provides a landscape-scale platform for assessing how directional changes in resource availability, which are expected and ongoing for most global change drivers (22), will affect ecosystem structure and function.

RESULTS AND DISCUSSION

Changes in soil hydraulics and pore systems

Shifts in the properties of large soil pores can be identified by changes in infiltration under near-saturated conditions. We therefore measured infiltration rates at pressure potentials close to saturation (−0.5, −1.5, −2.5, −3.5, and −5.5 hPa) in plots on both irrigated and control transects of

[1]Department of Environmental Sciences, Rutgers, The State University of New Jersey, New Brunswick, NJ 08901, USA. [2]Department of Architecture and Environmental Design, Temple University, Ambler, PA 19002, USA. [3]Department of Environmental Sciences, University of California, Riverside, Riverside, CA 92521, USA. [4]Department of Geography and Atmospheric Science, University of Kansas, Lawrence, KS 66045, USA. [5]Division of Biology, Kansas State University, Manhattan, KS 66506, USA. [6]Department of Biology and Graduate Degree Program in Ecology, Colorado State University, Fort Collins, CO 80523, USA.
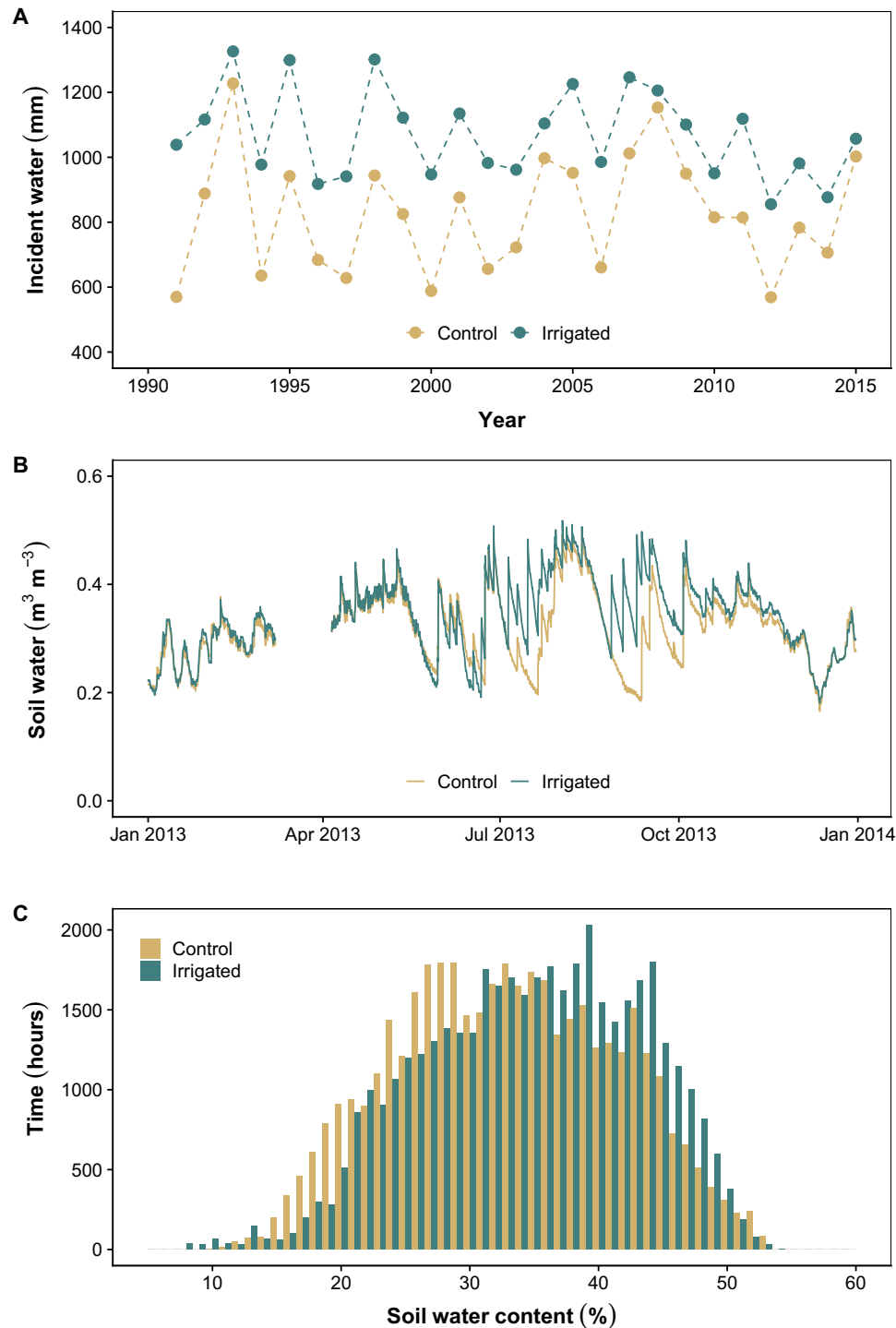*Corresponding author. Email: gimenez@envsci.rutgers.edu

Fig. 1. Characterization of experimental water regimes. (**A**) Total annual rainfall at the Konza Prairie Biological Station (Control) and total rainfall plus water applied as part of the ITE (Irrigated). (**B**) Volumetric soil water content (daily means across six sets of sensors) in control and irrigated transects for an example year. (**C**) Distribution of soil water content at the experimental site for an 8-year period (2008–2015).

the ITE. Further, because soil physical and chemical properties are often influenced by geomorphic processes, we evaluated soils at both upland and lowland landscape positions. Compared to the control, rainfall supplementation reduced mean infiltration rates by 21 to 33% in pores spanning 545 to 2000 μm [i.e., pressure potentials (h) spanning

−1.5 to −5.5 hPa; Fig. 2A]. The effect size and its strength of evidence (i.e., the standardized coefficient and its 95% confidence interval, respectively) varied across the range of pore sizes investigated but were greatest for pores approximately 850 μm in diameter (−3.5 hPa; table S2). There was no evidence that the properties of large pores differed

between upland and lowland soils or that landscape position moderated the effect of supplemental rainfall (table S2). Moreover, this decrease in infiltration rate was not accompanied by a decrease in soil porosity; high-precision measurements of the volume and mass of excavated soil

blocks indicated that total porosity increased with irrigation in the lowland while remaining constant in the upland (Fig. 2B and table S3).

Soil water retention is controlled by pores spanning a broad range of sizes (approximately 1 to 1000 μm in diameter), which implies that changes in pore systems will manifest as shifts in the relationship between the volume of water held by a soil and the pressure potential at which it is held (i.e., in water retention curves). Expression of independent and dependent variables is arbitrary for water retention curves such that curve shifts can be viewed as changes in either variable;
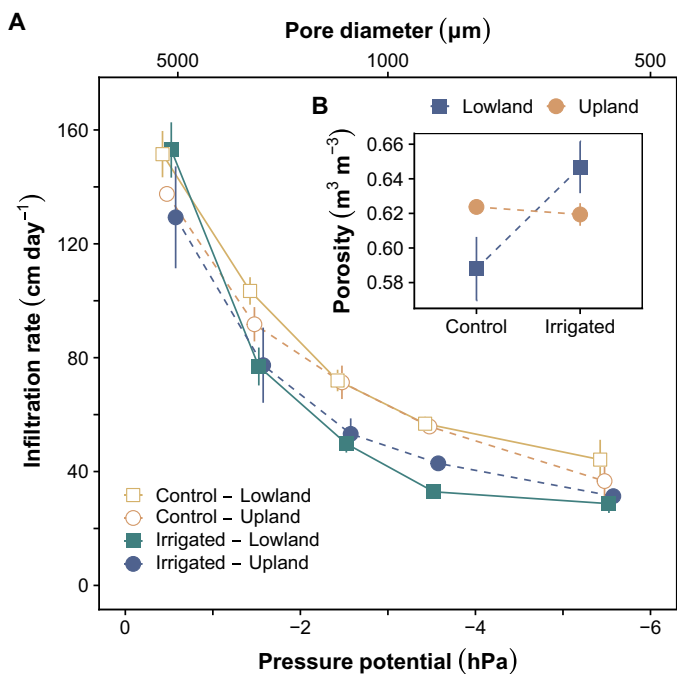

Fig. 2. Soil infiltration and porosity. (A) Infiltration rates (mean ± SE across pairs of plot-level values) at the five pressure potentials evaluated. Pore diameters are those of the largest pores transmitting water at the pressure potentials indicated. Outcomes of statistical evaluations are presented in table S1. (B) Total porosity of soil blocks (mean ± SE across block pairs). Statistical evaluations are summarized in tables S2 and S3. Horizontal offsets have been added to the points in (A) to reduce overlap.
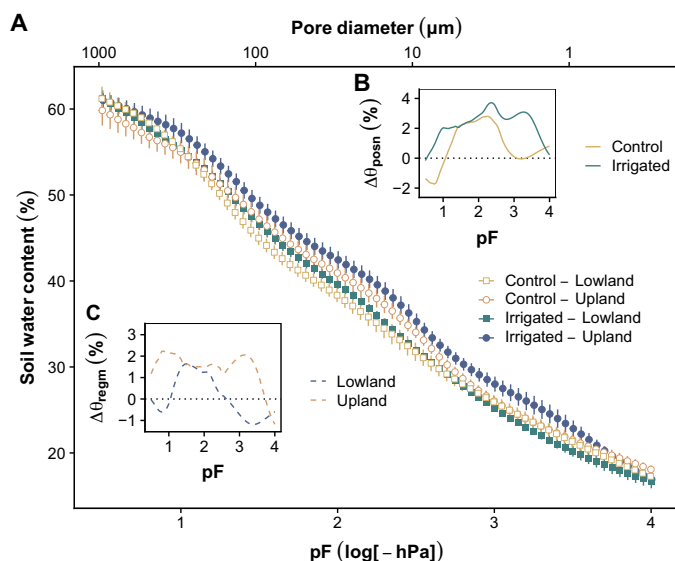
Fig. 3. Soil water retention properties. (A) Water retention curves from interpolated data (mean ± SE across four samples per treatment group). Insets show the sizes of predominant effects as the difference in water content ($\Delta\theta_v$) between (B) upland and lowland landscape positions and (C) irrigated and control water regimes, each calculated from the means in (A). Statistical evaluations are summarized in table S4.
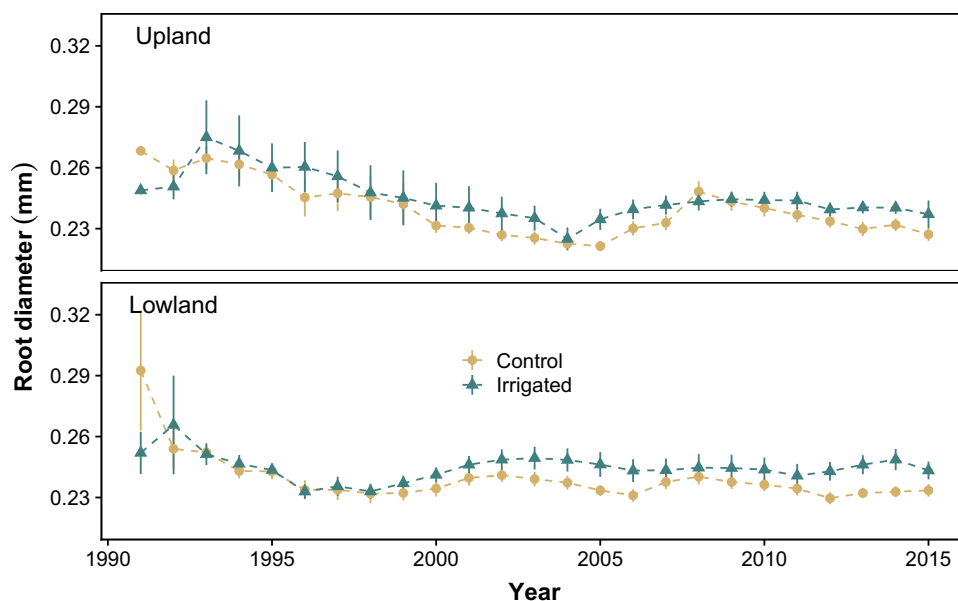

Fig. 4. CWM root diameter through the course of the ITE. Points depict means (±SE) across all plots within water regimes ($n = 5$ per regime in the first 2 years of the experiment but $n = 12$ subsequently). Statistical evaluations are summarized in table S5.

differences in θ_v are evaluated here. Using water retention data spanning pressure potentials of −3 to −10,000 hPa (evaluated here in terms of pF at intervals 0.5 units wide; pF = $\log_{10}[-h]$), we examined the individual and combined effects of rainfall supplementation and landscape position on water retained by various pore-size classes (Fig. 3A). Soils from the upland were capable of holding more water than were lowland soils; we denote the difference as $\Delta\theta_{posn}$, for which positive values indicate greater water retention in upland soils at a given pressure potential (Fig. 3B). The difference was greatest in pores approximately 10 to 30 μm in diameter, or pF = 2.0 to 2.5 (table S4), where $\Delta\theta_{posn}$ reached approximately 4% of the soil volume. Moreover, there was strong evidence that $\Delta\theta_{posn}$ was greater in irrigated than in control soils for pores >95 and <10 μm in diameter (i.e., intervals outside pF = 1.5 to 2.5; Fig. 3B and table S4); this difference varied with pF except over the interval 3.0 to 3.5.

The experimental increase in precipitation also induced changes in soil water retention, although the effect differed markedly by landscape position (Fig. 3C). In the upland, irrigated soils retained more water than control soils in pores 1 to 300 μm in diameter (i.e., pF intervals spanning 1.0 to 3.5; table S4). The average size of this effect, expressed as the difference in water retention between regimes ($\Delta\theta_{regm}$), corresponded to 1.7% of the soil volume across the range. The effect was weaker in the largest and smallest pore sizes investigated (300 to 1000 and 0.3 to 1.0 μm, or pF = 0.5 to 1.0 and 3.5 to 4.0, respectively), as reflected in the strong interaction effects with pF in these ranges (table S4). In the lowland, rainfall supplementation increased water retention mainly in pores 10 to 300 μm in diameter (pF = 1.0 to 2.5), with $\Delta\theta_{regm}$ averaging 1.0% of the soil volume (Fig. 3C). Outside of this range, $\Delta\theta_{regm}$ was negligible to slightly negative, possibly indicating that irrigation reduced the volume of pores 0.3 to 3.0 μm in diameter (pF from 3.0 to 4.0) in lowland soils.

Roots as a mechanism of change
A number of mechanisms could explain the shifts in infiltration, porosity, and water retention induced by increased precipitation in just two decades. We explored three prominent possibilities, beginning with the prospect that infiltration declined due to increased pore blockage by roots (13, 23). Consistent with this explanation, roots were slightly (2.7 to 6.8%) wider in plots receiving supplemental rainfall than they were in control plots [measured as the community-weighted mean (CWM) of fine-root diameter] during the 2011–2015 period (Fig. 4 and tables S1 and S5). Although CWM root diameter exhibited a similar trend in earlier periods (notably 2001–2010), the pattern weakened during years of high ambient rainfall (notably 2004 and 2008), especially in the upland. These results can be attributed, in large part, to the irrigated plant community's shift in dominance from one grass to another, for which the transition spanned approximately a decade (24). While the magnitude of the change in CWM root diameter was modest, the underlying data represent the central tendency of fine-root diameter distributions and it is likely that differences extended across the full range of these distributions.

In principle, an expansion of root system size (typically measured as length or biomass) could have contributed to pore blockage. Our porosity results suggest that, in the upland, root volumes did not change in response to rainfall supplementation, consistent with earlier findings that standing belowground biomass was unaffected by irrigation in the upland (24). In contrast, increased porosity in the lowland may correspond to greater belowground growth. Although root biomass was not measured directly in the lowland, aboveground plant biomass has
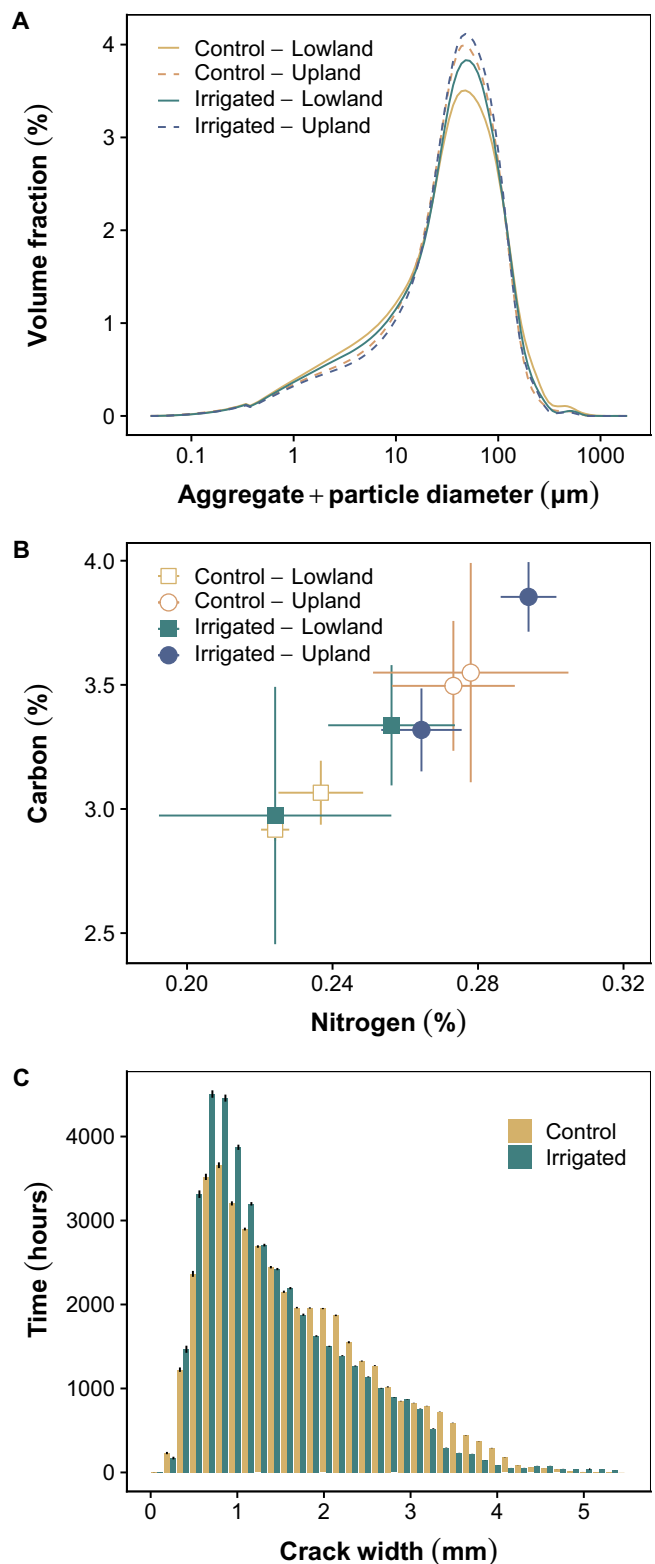
Fig. 5. Additional soil properties. (**A**) Size distribution of aggregates and fine particles in Konza Prairie soil (means of data aggregated to the plot level). (**B**) Soil carbon and nitrogen content (mean ± SE across triplicate samples in each of eight plots). (**C**) Estimated distribution of soil crack widths through eight growing seasons (bootstrapped mean ± SE). Statistical evaluations for (A) and (B) are summarized in tables S6 and S3, respectively.

responded 22% more strongly to increased water availability in that location, on average, since the study began (fig. S1), suggesting that an increase in belowground biomass likely occurred as well.

The changes in water retention we observed can, at least in part, be explained by increased clogging of pores by roots. Pore blockage typically manifests as a decrease in water retention in the range of pore sizes colonized by roots (as a result of a reduction in pore space) and an increase in water retention outside that range (due to both the formation of new pores and a reduction in the size of colonized pores) (13, 25). While the expected increase in water retention was observed (positive $\Delta\theta_{regm}$ at moderate pF), the reduction expected in irrigated plots was not (i.e., negative $\Delta\theta_{regm}$ at low pF; Fig. 3C). This suggests that roots were not the sole cause of the observed differences in water retention.

Aggregation as a mechanism of change

Changes in soil aggregation (i.e., the binding of soil particles and organic matter) could have induced the changes in soil hydraulic properties we observed if, for example, shifts in microbial activity altered aggregate formation and persistence (16, 26, 27). We therefore analyzed the size distributions of samples containing a combination of soil aggregates and individual particles. This analysis revealed only minor differences by irrigation regime (mainly in the 10- to 100-μm range) in addition to the expected pattern of slightly finer texture in the lowland (particularly the 1- to 10-μm range; Fig. 5A and table S6) (21).

Assuming that aggregates were more abundant than individual particles in the 10- to 100-μm-diameter range, the small, irrigation-induced increase in this range could be attributed to more extensive complex formation between clay particles and organic matter (10). Greater aggregate amounts in lowland soils may be further attributable to their modestly elevated carbon and nitrogen content (Fig. 5B and table S3). However, these changes did not measurably alter aggregate stability (tables S7 and S8) and were not of sufficient magnitude to have caused the changes in large pores associated with infiltration.

An additional possibility we investigated was that cations capable of dispersing aggregates were introduced by irrigation. We ruled this out, as the cation ratio of soil structural stability (CROSS) for groundwater at Konza Prairie spanning 1991–2014 (interannual mean ± SD = 0.17 ± 0.02 mol$^{0.5}$ m$^{-1.5}$) was well below the range at which dispersion occurs (28, 29) and only slightly elevated over CROSS measured in rainwater for the same period (0.04 ± 0.02 mol$^{0.5}$ m$^{-1.5}$) (fig. S2A). Similarly, the exchangeable dispersive percentage (EDP) of cations in soil samples collected during the study was not of sufficient magnitude to suggest that clay particles had been markedly dispersed (30); mean EDP was also not statistically differentiable between irrigated and control plots (fig. S2B, Table 1, and table S3).

Shrink-swell dynamics as a mechanism of change

Although most abiotic mechanisms act too slowly to induce substantial soil hydraulic changes on decadal time scales, it is possible that supplemental rainfall and the consequent reduction in soil water variability altered shrink-swell cycles. Changes to soil hydraulic properties would have arisen if less frequent or less intensive soil shrinkage diminished the sizes of cracks and other large pores. To evaluate this possibility, we modeled the distribution of crack sizes using water content records that spanned 8 years; we estimate that irrigation decreased the median width by 15%, from 1.48 to 1.25 mm, during this period (Fig. 5C). Pores on the order of 1.5-mm hold water at $h = -2$ hPa, indicating that they fall in the size and h range that the infiltration analysis indicated were most affected by rainfall supplementation. Moreover, the finding of wider cracks in control plots is also consistent with fluctuations in soil water content being greater in those plots (i.e., indicative of more intense shrink-swell cycles) (31). We note that altered shrink-swell cycles sustained over several years can induce nonreversible changes in pore system structure because of soil particle rearrangement (15, 32). While it is not clear if the size of this effect or that of changes in rooting patterns had a greater influence on the observed shifts in soil hydraulic properties, it is likely that they both contributed, perhaps even acting synergistically.

CONCLUSIONS

It is clear from this study and others that soil hydraulic properties can change over decadal time scales in response to shifts in climatic conditions (15, 16, 20). Given that directional precipitation regime shifts are likely to occur globally in the coming decades, appreciable soil structural alterations could occur over widespread regions, with important implications for water storage and fluxes. Changes in soil hydraulic properties could themselves have consequences for biogeochemical processes such as soil carbon storage and nitrogen fluxes (9). Moreover, these changes could induce feedbacks, for example, if altered water regimes affect key plant physiological processes or community dynamics and thereby lead to further shifts in soil pore systems.

In addition to characterizing the nature of soil hydraulic changes that may arise in response to various climatic shifts, it will be critical for future work to elucidate the biological, chemical, and physical mechanisms that mediate these changes. Here, we documented correlative evidence that two processes (shifts in rooting patterns and shrink-swell dynamics) may play important roles, but stronger, experimentally derived evidence will be needed to confirm causal relationships. Moreover, it is likely that the mechanisms altering pore systems will vary as a function of the environmental setting. As one study showed, the aggregate properties of a sandy soil responded very differently to

Table 1. Cation concentrations and the EDP (mean ± SE) of soils from the ITE.

Water regime	Landscape position	Na (cmol$_c$ kg^{-1})	K (cmol$_c$ kg^{-1})	Ca (cmol$_c$ kg^{-1})	Mg (cmol$_c$ kg^{-1})	EDP (%)
Control	Lowland	0.19 ± 0.02	1.27 ± 0.08	26.24 ± 1.16	5.80 ± 0.45	3.50 ± 0.18
Control	Upland	0.18 ± 0.03	1.35 ± 0.10	19.92 ± 0.40	6.97 ± 0.22	3.72 ± 0.14
Irrigated	Lowland	0.30 ± 0.05	1.26 ± 0.08	26.23 ± 0.75	6.26 ± 0.38	3.88 ± 0.22
Irrigated	Upland	0.24 ± 0.04	1.52 ± 0.06	23.12 ± 0.43	6.93 ± 0.36	4.21 ± 0.22

elevated CO_2 depending on nitrogen availability, likely due to differences in the availability of labile organic matter (16). It will also be important to determine how malleable soils with different textures and mineral compositions are when acted upon by various climatic drivers.

The findings of this research also raise the possibility that land surface models may need to account for shifts in soil hydraulic properties to accurately project water storage and fluxes under future climate regimes. The vast majority of models currently assume that water retention, infiltration, and other properties vary strictly with soil texture and depth, remaining constant through time (1). Our results suggest that, in the near term, it would be prudent to assess the sensitivity of models to shifts in soil hydraulic properties. Longer-term, predicting such shifts may be viable if the dynamics of the processes affecting soil hydraulic properties can be characterized. Defining these controls is therefore an important area of future research and will be critical to determining how to improve the accuracy of land surface model projections.

MATERIALS AND METHODS
Field experiment and site
This study builds on the ITE (33) at the Konza Prairie Biological Station in Kansas, USA (39.091°N, 96.613°W). The region has a continental climate with a mean annual air temperature of 12.8°C and a mean annual precipitation rate of 835 mm; approximately 75% of precipitation falls as rain during the growing season. The ITE is composed of four 140-m transects extending from the upland to the lowland prairie; they span an elevation range of 7 m. Between 1991 and 2017, two of the four transects were irrigated during the growing season with local groundwater to a depth sufficient to match potential evapotranspiration for May to September (33); the two remaining transects were left nonirrigated as controls. Supplemental rainfall was applied via a series of stationary sprinklers with rotating heads (10-m separation) positioned along the two irrigated transects. Sprinklers were 1.0 m tall and delivered water over circular areas 30 m in diameter (21). Irrigation amounts were highly consistent within 6 m of the line of sprinklers (33), and it was within this zone that infiltration measurements and soil sampling took place. Over the 22 years before the soil measurements described here, control transects received an average of 823 mm of rain, while irrigated transects received 1085 mm (Fig. 1A).

Vegetation at the site of the ITE is dominated by grasses and forbs (especially *Andropogon gerardii* and *Panicum virgatum*), although some short-statured shrubs are also present (e.g., *Amorpha canescens*) (table S1). Supplemental rainfall increased aboveground net primary productivity (ANPP) in nearly all years of the experiment (fig. S1); belowground productivity has not routinely been measured. The effect of rainfall supplementation on ANPP was most often greater in the lowland than in the upland, attributable to lowland soils being deeper and therefore allowing greater water storage and root growth.

Given that frequent fire is a natural component of this ecosystem and required for it to persist (34), aboveground plant material across much of Konza Prairie is burned before new growth occurs each spring. Most of the ash is removed from the site by wind (during burns or subsequently), although some enters the soil profile during rain events. However, control and irrigated transects were collocated and burned simultaneously, so any differences in soil structure described here cannot be attributed to cations introduced by ash. Also, soil pH measurements from sites across the Konza Prairie Biological Station indicate that annual fires do not alter soil pH (35).

Soils at the site are silty clay loams; most are part of the Clime-Sogn complex, although the lowland is transitional to the Irwin series (36). The Clime series is a fine, mixed, active, mesic Udorthentic Haplustoll, while the Sogn series is a loamy, mixed, superactive, mesic Lithic Haplustoll. In contrast, the Irwin series is a fine, mixed, superactive, mesic Pachic Argiustoll. The underlying geology is dominated by limestone interbedded with shale.

Soil hydraulic properties
Measurements of infiltration were carried out in situ in July 2013. Infiltration runs were conducted at the upland and lowland landscape positions of each of the four transects in the ITE ($n = 15$ runs at each of eight locations) spanning four consecutive rain-free days. Transects thus served as blocks in which two sampling locations were established per transect. Before runs, ≤10 minidisk infiltrometers (METER Environment, Pullman, USA) were set up in a 2 × 2 m area near the center line of transects. Spatial clustering was necessary to minimize trampling of experimental plots and because infiltrometers were fitted with pressure transducers that fed data to a CR23X data logger (Campbell Scientific, Logan, USA). During runs, infiltrometers were held at each of five pressure potentials (−0.5, −1.5, −2.5, −3.5, and − 5.5 hPa) for approximately 30 min, while water was released into the soil ($n = 600$ infiltration measurements in total); water level was recorded at 3-s intervals. Infiltration rates were computed from smoothed data when steady state was achieved (77% of measurements after data cleaning). Data were smoothed using the Savitzky-Golay method with 3-min windows ($n = 40$ values per window). Infiltration rates were subsequently corrected to 20°C by accounting for temperature effects on the viscosity and density of water.

Soil cores were used for characterizing water retention. Two cores (8 cm diameter × 5 cm height) were collected from each of the eight sampling locations and returned to the laboratory intact. A HYPROP system (METER Environment, Pullman, USA) was used to measure volumetric water content (θ_v) at pressure potentials spanning −3 to −1000 hPa, while a WP4C system (METER Environment, Pullman, USA) was used for pressure potentials spanning −1000 to −10,000 hPa. Data were then fitted with smoothing splines such that θ_v could be determined at equivalent pressure potentials across the full measured range.

The maximum diameter of pores (d) holding water at a given pressure potential (h) was determined using the Young-Laplace equation (37), which can be expressed as

$$d = \frac{4\gamma \cos \alpha}{\rho g \mid h \mid} \tag{1}$$

where γ is the surface tension of water (0.0728 J m^{-2} at 20°C), α is the apparent contact angle between water and the pore (assumed to be zero), ρ is the density of water (1000 kg m^{-3}), g is the gravitational constant (9.81 m s^{-2}), and h is the pressure potential. This relationship assumes that pores are circular in cross section. Given values of h in hPa, equivalent diameters in micrometers were calculated from Eq. 1.

Root diameter
CWMs of fine-root diameter were used to determine if shifts in soil hydraulic properties could potentially be explained by roots filling greater fractions of soil pore systems. Species-level root diameter data came from the TRY Plant Trait Database version 5 (38), which contains records from several sources including the Fine-Root Ecology Database

(39). TRY was queried for records matching the names of all plant species at Konza Prairie (after taxonomic standardization). The geometric mean was used to aggregate records of fine-root diameter at the species level (n = 1 to 60 per species, 1102 in total); 62 species and 88 ± 4% of cover (mean ± SD across years) were represented in the resulting dataset. Genus-level values were then added for species without fine-root diameter data in TRY and for plant taxa only identifiable to the genus level in the field surveys described below. Genus-level values were likewise computed as geometric means of the relevant diameter data, but the starting point was a previously derived, gap-filled version of the Fine-Root Ecology Database (11). Ninety-three species and 98 ± 2% of cover were accounted for in the final dataset. Next, the relative abundance of each species was computed at the plot scale on an annual basis using data from surveys of plant cover that took place between 1991 and 2015; these served as weights when calculating CWMs. Vegetation was surveyed annually in circular plots (10 m^2) that were positioned along the four experimental transects (n = 12 upland and 12 lowland plots, except in 1991–1992, when n = 5 upland and 5 lowland plots). Cover was measured using a modified Daubenmire classification, with the midpoints of each cover class (0 to 1%, 1 to 5%, 5 to 25%, 25 to 50%, 50 to 75%, 75 to 95%, or 95 to 100%) used in calculations of relative abundance. In addition, species cover was measured shortly after soil sampling at the eight locations described above. In this effort, cover was measured to within ~1% of the actual value in four replicate plots. Once the root diameter dataset was joined to each of the cover datasets, species cover values were relativized to the total cover in the relevant plot (table S1). Weighted means of diameters were then computed at the plot level for each year of the study.

Additional soil characteristics

Triplicate soil samples were taken from each of the eight sampling locations (n = 24 samples) for further characterization. Samples were collected from the surficial 5 cm of soil in July 2013 and chilled (4°C) until they were subsampled for analyses. Three subsamples per sample (n = 72) were dried and analyzed for total carbon and nitrogen content using a vario MAX cube CN analyzer (Elementar Americas, Mt. Laurel, USA) with helium as a carrier gas. Additional subsamples (n = 72) were dried, lightly ground, and analyzed for the size distribution of aggregates and fine particles via laser diffraction (LS-13-320, Beckman Coulter, Indianapolis, USA). Aggregate stability was analyzed using a wet sieving apparatus (Eijkelkamp Soil & Water, Gelderland, The Netherlands) containing four sieves (2.0-, 1.0-, 0.25-, and 0.053-mm openings). Samples were measured in duplicate (n = 16 per sieve size), although one sample with anomalously high passage was excluded from the statistical analysis (n = 63 in total). An additional soil block (2000 to 2500 cm^3) was sampled from each plot for measurements of total porosity. Blocks were scanned using multistripe laser triangulation (40) to determine volumes (n = 8). Dry masses were determined in triplicate subsamples taken from each block and averaged.

The frequency of crack formation in soils experiencing control versus supplemental precipitation was determined in two steps. First, the relationship between crack development in the soil surface as a function of decreasing θ_v was characterized. This was done using three soil cores with known surface areas (50 cm^2) when saturated; cores were from the Clime-Sogn complex but not from the ITE. Color images and core mass measurements were taken at 7 to 11 time points while cores were dried under ambient laboratory conditions over the course of several weeks. Core mass was used to calculate θ_g, which was translated to θ_v using final measurements of core bulk density. The relationship between

mean crack width and θ_v was then characterized using smoothing splines fitted to bootstrapped samples of the data (n = 1000 iterations; smoothing parameter = 0.7) (fig. S3). Second, the resulting functions were applied to mean time series of θ_v measured via time domain reflectometry (TDR) at 30-min intervals during the 2008–2015 growing seasons. TDR data were collected at three locations in each combination of water regime and landscape position (n = 12), with probes extending vertically through the 15 cm of soil nearest the surface.

CROSS (cation ratio of structural stability) was used to assess the potential for the groundwater used in irrigation to alter soil structure by dispersing or flocculating clays (28). CROSS values for groundwater were compared to those for rainwater and published relationships between CROSS and clay dispersion (28, 29). CROSS was calculated as

$$\text{CROSS} = \frac{[\text{Na}] + 0.56[\text{K}]}{\sqrt{\frac{[\text{Ca} + 0.60[\text{Mg}]}{2}}} \qquad (2)$$

where concentrations are in mmol$_c$ liter^{-1}. The dataset on groundwater chemistry included measurements spanning 1991–2014 from a set of wells approximately 3 km from the source of irrigation water (41). The dataset on rainwater chemistry came from a National Atmospheric Deposition Program station (NTN site KS31) approximately 0.25 km from the experimental site; data for the same time span were extracted. In both cases, the mean and SD of all measurements taken within a given year (n = 14 to 107 per year for groundwater and n = 20 to 54 per year for rainwater) were determined after averaging replicate measurements, if present. The dispersive capacity of cations adsorbed to soils at the study site was assessed using the EDP

$$\text{EDP} = \frac{[\text{Na}] + 0.556[\text{K}] + 0.037[\text{Mg}]}{\text{CEC}} \times 100 \qquad (3)$$

where CEC is the cation exchange capacity and concentrations are in cmol$_c$ kg^{-1} (29). Cations were measured from ammonium acetate extracts of each soil sample (n = 24) and analyzed using an iCAP-7000 ICP-OES system (Thermo Fisher, Waltham, USA) with a liquid argon carrier. The CEC value used was the mean of those reported for the Clime and Sogn series by the National Resource Conservation Service (33.6 cmol$_c$ kg^{-1}). This value was similar to the sum of [Na], [K], [Ca], and [Mg] in our samples (31.9 cmol$_c$ kg^{-1}), confirming that methodological differences did not affect the comparability of measurements.

Data analysis

The potential effects of precipitation regime and landscape position on response variables (i.e., soil hydraulic properties and other characteristics measured at the eight sampling locations) were investigated through mixed-effects linear modeling. In the cases of soil porosity, carbon, nitrogen, and EDP, models were fit with all data records included. However, subsets of data were used in models of infiltration rate (subsetted by pressure potential), θ_v (divided into intervals of 0.5 pF units (log$_{10}$[−hPa]), particle size [divided into intervals of integer log$_{10}$(μm) units], aggregate stability (subsetted by sieve size), and CWM root diameter (divided into 5-year intervals). This allowed us to estimate the effect sizes of precipitation and landscape position on response variables in the absence of nonlinear effects of pressure potential, pF, particle/aggregate diameter, or community transitions. In the analyses of infiltration rate and particle size, data were log-transformed to achieve residual normality. Precipitation, landscape position, and

their interaction were entered into models as fixed-effects terms. Random-effects terms were also included to account for variation due to transect identity and interactions with precipitation regime and landscape position, as well as for repeated measurements within plots and samples, if applicable. Continuous variables were standardized by two SDs, while discrete variables with two levels were coded as ±0.5, making all coefficients comparable in scale (42). Rather than using binary indicators of significance (i.e., P values) to gauge the importance of model terms, we evaluated terms' effect sizes and the strength of evidence that their coefficients were nonzero (43). Effect sizes were determined from the absolute values of model-averaged coefficients, with larger deviations from zero being indicative of greater effects. Model averaging involved fitting the full model, all hierarchically complete reduced models, and the intercept-only model. For model variants that had corrected Akaike information criteria (AIC$_c$) scores sufficiently close to the variant with the smallest AIC$_c$ (ΔAIC$_c$ < 6), standardized coefficients for all retained fixed-effect terms were averaged. Evidence of an effect being nonzero was considered strong when the 95% confidence interval of the corresponding standardized, model-averaged coefficient excluded zero.

SUPPLEMENTARY MATERIALS

Supplementary material for this article is available at http://advances.sciencemag.org/cgi/content/full/5/9/eaau6635/DC1

Fig. S1. Aboveground net primary productivity.
Fig. S2. Metrics of cation dispersive capacity.
Fig. S3. Relationship between soil crack widths and water content.
Table S1. Plant community composition.
Table S2. Statistical modeling summary for infiltration rate.
Table S3. Statistical modeling summary for various soil properties.
Table S4. Statistical modeling summary for water retention.
Table S5. Statistical modeling summary for root diameter.
Table S6. Statistical modeling summary for soil aggregates and particles.
Table S7. Statistical modeling summary for aggregate stability.
Table S8. Aggregate stability.

REFERENCES AND NOTES

1. H. Vereecken, A. Schnepf, J. W. Hopmans, M. Javaux, D. Or, T. Roose, J. Vanderborght, M. H. Young, W. Amelung, M. Aitkenhead, S. D. Allison, S. Assouline, P. Baveye, M. Berli, N. Brüggemann, P. Finke, M. Flury, T. Gaiser, G. Govers, T. Ghezzehei, P. Hallett, H. J. H. Franssen, J. Heppell, R. Horn, J. A. Huisman, D. Jacques, F. Jonard, S. Kollet, F. Lafolie, K. Lamorski, D. Leitner, A. McBratney, B. Minasny, C. Montzka, W. Nowak, Y. Pachepsky, J. Padarian, N. Romano, K. Roth, Y. Rothfuss, E. C. Rowe, A. Schwen, J. Šimůnek, A. Tiktak, J. Van Dam, S. E. A. T. M. van der Zee, H. J. Vogel, J. A. Vrugt, T. Wöhling, I. M. Young, Modeling soil processes: Review, key challenges, and new perspectives. Vadose Zone J. 15, 1–57 (2016).
2. K. W. Watson, R. J. Luxmoore, Estimating macroporosity in a forest watershed by use of a tension infiltrometer. Soil Sci. Soc. Am. J. 50, 578–582 (1986).
3. M. A. Cregger, C. W. Schadt, N. G. McDowell, W. T. Pockman, A. T. Classen, Response of the soil microbial community to changes in precipitation in a semiarid ecosystem. Appl. Environ. Microbiol. 78, 8587–8594 (2012).
4. H. Jenny, C. D. Leonard, Functional relationships between soil properties and rainfall. Soil Sci. 38, 363–382 (1934).
5. B. W. Stewart, R. C. Capo, O. A. Chadwick, Effects of rainfall on weathering rate, base cation provenance, and Sr isotope composition of Hawaiian soils. Geochim. Cosmochim. Acta 65, 1087–1099 (2001).
6. K. A. Lohse, W. E. Dietrich, Contrasting effects of soil development on hydrological properties and flow paths. Water Resour. Res. 41, W12419 (2005).
7. T. Głąb, Effect of soil compaction and N fertilization on soil pore characteristics and physical quality of sandy loam soil under red clover/grass sward. Soil Till. Res. 144, 8–19 (2014).
8. Y. Hayashi, K. Ken'ichirou, T. Mizuyama, Changes in pore size distribution and hydraulic properties of forest soil resulting from structural development. J. Hydrol. 331, 85–102 (2006).
9. S. I. Seneviratne, T. Corti, E. L. Davin, M. Hirschi, E. B. Jaeger, I. Lehner, B. Orlowsky, A. J. Teuling, Investigating soil moisture–climate interactions in a changing climate: A review. Earth Sci. Rev. 99, 125–161 (2010).
10. C. J. Bronick, R. Lal, Soil structure and management: A review. Geoderma 124, 3–22 (2005).
11. J. S. Caplan, S. J. Meiners, H. Flores-Moreno, M. L. McCormack, Fine-root traits are linked to species dynamics in a successional plant community. Ecology 100, e02588 (2019).
12. A. Volder, R. M. Gifford, J. R. Evans, Effects of elevated atmospheric CO$_2$, cutting frequency, and differential day/night atmospheric warming on root growth and turnover of Phalaris swards. Glob. Chang. Biol. 13, 1040–1052 (2007).
13. P. Scholl, D. Leitner, G. Kammerer, W. Loiskandl, H.-P. Kaul, G. Bodner, Root induced changes of effective 1D hydraulic properties in a soil column. Plant Soil 381, 193–213 (2014).
14. A. B. De-Campos, A. I. Mamedov, C.-h. Huang, Short-term reducing conditions decrease soil aggregation. Soil Sci. Soc. Am. J. 73, 550–559 (2009).
15. D. A. Robinson, S. B. Jones, I. Lebron, S. Reinsch, M. T. Domínguez, A. R. Smith, D. L. Jones, M. R. Marshall, B. A. Emmett, Experimental evidence for drought induced alternative stable states of soil moisture. Sci. Rep. 6, 20018 (2016).
16. J. S. Caplan, D. Giménez, V. Subroy, R. J. Heck, S. A. Prior, G. B. Runion, H. A. Torbert, Nitrogen-mediated effects of elevated CO$_2$ on intra-aggregate soil pore structure. Glob. Chang. Biol. 23, 1585–1597 (2017).
17. M. C. Rillig, S. F. Wright, M. F. Allen, C. B. Field, Rise in carbon dioxide changes soil structure. Nature 400, 628 (1999).
18. S. A. Prior, G. B. Runion, H. A. Torbert, H. H. Rogers, Elevated atmospheric CO$_2$ in agroecosystems: Soil physical properties. Soil Sci. 169, 434–439 (2004).
19. H. Lavee, P. Sarah, A. C. Imeson, Aggregate stability dynamics as affected by soil temperature and moisture regimes. Geogr. Ann. Ser. B 78, 73–82 (2017).
20. D. R. Hirmas, D. Giménez, A. Nemes, R. Kerry, N. A. Brunsell, C. J. Wilson, Climate-induced changes in continental-scale soil macroporosity may intensify water cycle. Nature 561, 100–103 (2018).
21. A. K. Knapp, J. M. Briggs, J. K. Koelliker, Frequency and extent of water limitation to primary production in a mesic temperate grassland. Ecosystems 4, 19–28 (2001).
22. M. D. Smith, A. K. Knapp, S. L. Collins, A framework for assessing ecosystem dynamics in response to chronic resource alterations induced by global change. Ecology 90, 3279–3289 (2009).
23. K. P. Barley, The root growth of irrigated perennial pastures and its effect on soil structure. Aust. J. Agr. Res. 4, 283–291 (1953).
24. K. R. Wilcox, J. M. Blair, A. K. Knapp, Stability of grassland soil C and N pools despite 25 years of an extreme climatic and disturbance regime. J. Geophys. Res. Biogeosci. 121, 1934–1945 (2016).
25. C. W. W. Ng, J. J. Ni, A. K. Leung, Z. J. Wang, A new and simple water retention model for root-permeated soils. Géotech. Lett. 6, 106–111 (2016).
26. M. Dorodnikov, E. Blagodatskaya, S. Blagodatsky, S. Marhan, A. Fangmeier, Y. Kuzyakov, Stimulation of microbial extracellular enzyme activities by elevated CO$_2$ depends on soil aggregate size. Glob. Chang. Biol. 15, 1603–1614 (2009).
27. J. M. Oades, The role of biology in the formation, stabilization and degradation of soil structure. Geoderma 56, 377–400 (1993).
28. P. Rengasamy, A. Marchuk, Cation ratio of soil structural stability (CROSS). Soil Res. 49, 280–285 (2011).
29. P. Rengasamy, E. Tavakkoli, G. K. McDonald, Exchangeable cations and clay dispersion: Net dispersive charge, a new concept for dispersive soil. Eur. J. Soil Sci. 67, 659–665 (2016).
30. J. M. Bennett, A. Marchuk, S. Marchuk, An alternative index to the exchangeable sodium percentage for an explanation of dispersion occurring in soils. Soil Res. 54, 949–957 (2016).
31. G. Bodner, P. Scholl, H.-P. Kaul, Field quantification of wetting–drying cycles to predict temporal changes of soil pore size distribution. Soil Tillage Res. 133, 1–9 (2013).
32. A. S. Gregory, C. R. Webster, C. W. Watts, W. R. Whalley, C. J. A. Macleod, A. Joynes, A. Papadopoulos, P. M. Haygarth, A. Binley, M. W. Humphreys, L. B. Turner, L. Skot, G. P. Matthews, Soil management and grass species effects on the hydraulic properties of shrinking soils. Soil Sci. Soc. Am. J. 74, 753–761 (2010).
33. A. K. Knapp, J. K. Koelliker, J. T. Fahnestock, J. M. Briggs, Water relations and biomass responses to irrigation across a topographic gradient in tallgrass prairie, paper presented at the 13th North American Prairie Conference, Windsor, Ontario, Canada, 6 to 9 August 1992.
34. A. Knapp, J. Briggs, D. Hartnett, S. Collins, Grassland Dynamics: Long-Term Ecological Research in Tallgrass Prairie (Oxford Univ. Press, 1998), 364 pp.
35. C. M. Carson, L. H. Zeglin, Long-term fire management history affects N-fertilization sensitivity, but not seasonality, of grassland soil microbial communities. Soil Biol. Biochem. 121, 231–239 (2018).
36. Natural Resources Conservation Service, U.S. Department of Agriculture, Web Soil Survey; https://websoilsurvey.nrcs.usda.gov/ [accessed 6 May 2018].
37. A. W. Adamson, Physical Chemistry of Surfaces (Wiley, 1982).

38. J. Kattge, S. Díaz, S. Lavorel, I. C. Prentice, P. Leadley, G. Bönisch, E. Garnier, M. Westoby, P. B. Reich, I. J. Wright, J. H. C. Cornelissen, C. Violle, S. P. Harrison, P. M. Van Bodegom, M. Reichstein, B. J. Enquist, N. A. Soudzilovskaia, D. D. Ackerly, M. Anand, O. Atkin, M. Bahn, T. R. Baker, D. Baldocchi, R. Bekker, C. C. Blanco, B. Blonder, W. J. Bond, R. Bradstock, D. E. Bunker, F. Casanoves, J. Cavender-Bares, J. Q. Chambers, F. S. Chapin III, J. Chave, D. Coomes, W. K. Cornwell, J. M. Craine, B. H. Dobrin, L. Duarte, W. Durka, J. Elser, G. Esser, M. Estiarte, W. F. Fagan, J. Fang, F. Fernández-Méndez, A. Fidelis, B. Finegan, O. Flores, H. Ford, D. Frank, G. T. Freschet, N. M. Fyllas, R. V. Gallagher, W. A. Green, A. G. Gutierrez, T. Hickler, S. I. Higgins, J. G. Hodgson, A. Jalili, S. Jansen, C. A. Joly, A. J. Kerkhoff, D. Kirkup, K. Kitajima, M. Kleyer, S. Klotz, J. M. H. Knops, K. Kramer, I. Kühn, H. Kurokawa, D. Laughlin, T. D. Lee, M. Leishman, F. Lens, T. Lenz, S. L. Lewis, J. Lloyd, J. Llusià, F. Louault, S. Ma, M. D. Mahecha, P. Manning, T. Massad, B. E. Medlyn, J. Messier, A. T. Moles, S. C. Müller, K. Nadrowski, S. Naeem, Ü. Niinemets, S. Nöllert, A. Nüske, R. Ogaya, J. Oleksyn, V. G. Onipchenko, Y. Onoda, J. Ordoñez, G. Overbeck, W. A. Ozinga, S. Patiño, S. Paula, J. G. Pausas, J. Peñuelas, O. L. Phillips, V. Pillar, H. Poorter, L. Poorter, P. Poschlod, A. Prinzing, R. Proulx, A. Rammig, S. Reinsch, B. Reu, L. Sack, B. Salgado-Negret, J. Sardans, S. Shiodera, B. Shipley, A. Siefert, E. Sosinski, J.-F. Soussana, E. Swaine, N. Swenson, K. Thompson, P. Thornton, M. Waldram, E. Weiher, M. White, S. White, S. J. Wright, B. Yguel, S. Zaehle, A. E. Zanne, C. Wirth, TRY—A global database of plant traits. *Glob. Chang. Biol.* **17**, 2905–2935 (2011).

39. C. M. Iversen, A. S. Powell, M. L. McCormack, C. B. Blackwood, G. T Freschet, J. Kattge, C. Roumet, D. B. Stover, N. A. Soudzilovskaia, R. Fisher, Fine-Root Ecology Database (FRED): A Global Collection of Root Trait Data with Coincident Site, Vegetation, Edaphic, and Climatic Data, Version 1 (2017).

40. D. R. Hirmas, D. Giménez, V. Subroy, B. F. Platt, Fractal distribution of mass from the millimeter- to decimeter-scale in two soils under native and restored tallgrass prairie. *Geoderma* **207–208**, 121–130 (2013).

41. G. Macpherson, AGW01 Long-term measurement of groundwater physical and chemical properties from wells on watershed N04D at Konza Prairie (2018); doi:10.6073/pasta/1bc227b976c83e0a8071f72cbc8fa19b.

42. A. Gelman, Scaling regression inputs by dividing by two standard deviations. *Stat. Med.* **27**, 2865–2873 (2008).

43. K. P. Burnham, D. R. Anderson, *Model Selection and Multimodel Inference: A Practical Information-Theoretic Approach* (Springer-Verlag, ed. 2, 2002).